Electrochemistry Communications 103 (2019) 7–11

Contents lists available at ScienceDirect

Electrochemistry Communications

journal homepage: www.elsevier.com/locate/elecom

Full communication

Electrochemical deposition of silicon from a sulfolane-based electrolyte: Effect of applied potential

Steffen Link[a], Svetlozar Ivanov[a,*], Anna Dimitrova[b], Stefan Krischok[b], Andreas Bund[a]

[a] Technische Universität Ilmenau, Electrochemistry and Electroplating Group, Gustav-Kirchhoff-Straße 6, 98693 Ilmenau, Germany
[b] Institute of Physics and Institute of Micro- and Nanotechnologies, MacroNano, Technische Universität Ilmenau, Ilmenau 98693, Germany

ARTICLE INFO

Keywords:
Sulfolane
Silicon deposition
Quartz crystal microbalance
Frequency damping
Copper silicide

ABSTRACT

As a low-cost, non-volatile, highly polar and chemically stable solvent, sulfolane has a high implementation potential for electroplating in organic media. This is the first report of the electrodeposition of silicon from sulfolane-based electrolytes. Voltammetric and chronoamperometric techniques, coupled with a quartz crystal microbalance, have been used to perform and characterize the process. Resonance frequency, f, damping, w, and apparent molar mass, M_{app} are used as sensitive parameters for the evaluation of the silicon layer formation. Si electrodeposition displays a strong dependence on the applied potential. Close to theoretical values for M_{app} and minimal w are observed at low deposition overpotentials, which allow an in situ quantitative mass evaluation. At higher overpotentials the process efficiency decreases due to simultaneous electrolyte decomposition. The electrodeposition of elemental Si (approx. 60% of the entire Si content) is evidenced by X-ray photoelectron spectroscopy. Additionally, the formation of a binary metal compound with the Cu substrate might be a key factor in the very good adhesion and mechanical stability of the layer.

1. Introduction

Elemental silicon is one of the most important materials in modern society, finding multiple applications in the electronics industry, solar cell production technology and electrochemical energy storage [1,2]. Si electrodeposition cannot be realized in water-based electrolytes due to its very low reduction potential and the high reactivity of the Si precursors. As a result, a large number of unconventional media, including high-temperature molten salts (HTMS) [3,4] and organic electrolyte solutions [5–22], has been suggested for this purpose.

The room-temperature organic electrolytes applied for Si deposition are based on propylene carbonate [5–10], tetrahydrofuran [10–13], acetonitrile [10–12,14], dichloromethane [14] and ionic liquids [15–22]. Although offering the possibility to deposit elemental Si, these electrolytes display certain drawbacks. Serious precautions must be taken when using electrolytes containing volatile solvents, since they have a high vapor pressure and are very flammable. The HTMS require high energy consumption and are extremely reactive. Room-temperature ionic liquids (RTIL) display low volatility, reduced flammability and have a large potential window of stability. However, most RTILs are expensive and electrodeposition from these electrolytes characteristically features solvent impurities incorporated in the silicon deposit [19,20]. Moreover, in some cases IL decomposition products are detected in the layer structure [20,21]. Considerable deposit contamination due to electrolyte decomposition has been observed as well for silicon deposition from propylene carbonate [9,10] and acetonitrile-based solutions [11].

Sulfolane, which is rarely used in electrochemical applications, has a remarkable chemical and thermal stability, high polarity and a very low protolithic constant [23]. Therefore, this compound can be used as a medium in which to perform many chemical processes affected by the reactivity of conventional solvents. In addition, sulfolane is an environmental friendly substance, displaying a low vapor pressure and minimal toxicity [23]. To the best of our knowledge, the application of sulfolane as a solvent for Si electrodeposition has not been approached so far. Therefore, in this work we aim to present the first study on the electrochemical deposition of Si from sulfolane-based electrolytes. Linear sweep voltammetry and chronoamperometry, coupled with quartz crystal microbalance (QCM) measurements, have been used to perform and characterize the deposition process. The chemical composition of the resulting deposit is analyzed by X-ray photoelectron spectroscopy (XPS). With the perspective of testing the deposited Si directly as an anode in Li-ion batteries, we chose a Cu substrate for our study.

* Corresponding author.
E-mail address: svetlozar.dimitrov.ivanov@tu-ilmenau.de (S. Ivanov).

https://doi.org/10.1016/j.elecom.2019.04.008
Received 22 March 2019; Received in revised form 11 April 2019; Accepted 12 April 2019
Available online 13 April 2019

2. Experimental

2.1. Chemicals and materials

Sulfolane and silicon tetrachloride (purification grade 99%) were both purchased from Alfa Aesar. Tetrabutylammonium chloride (TBACl, purification grade ≥ 97%), obtained from Sigma Aldrich, served as supporting electrolyte salt. Sulfolane was dried at 50 °C with a molecular sieve (pore diameter 0.3 nm, CarlRoth, Germany) for 3 days before 0.1 M TBACl was added to the solvent and then the solution was dried for another two days. 0.5 M $SiCl_4$ served as a precursor for silicon electrodeposition.

2.2. Electrochemical and quartz crystal microbalance experiments

All experiments were performed in an argon-filled glove box (MBraun UNIlab LMF auto) with O_2 and H_2O contents below 0.1 ppm at room temperature (25 °C). Linear sweep voltammetry, potentiostatic deposition and QCM measurements were accomplished in a lab-made PTFE cell. The Cu working electrode was polished with a silicon carbide paper (corn size 5 µm), rinsed with ethanol, dried in an argon atmosphere for 30 min before use and clamped via an O-ring (NB70) to the cell (0.20 cm^2 geometric area). A Pt plate, used as counter electrode, was heated to glowing red before each experiment. Throughout this work, the potential is presented against a homemade Ag/AgCl reference electrode, prepared for sulfolane, based on a publication by Saheb et al. [24]. 0.1 M TBACl dissolved in sulfolane was used as an electrolyte for the reference electrode. This was calibrated against fc/fc^+ (2.5 mM) in sulfolane with 0.2 M [BMP][TFSI] as supporting electrolyte (E = 787 mV vs. fc/fc^+). Electrochemical measurements were carried out with a multi-channel potentiostat (VMP 3) from Bio-Logic Scientific Instruments. Immediately after deposition the samples were thoroughly washed with propylene carbonate and dried for 1 h under argon.

For the QCM measurements, a Cr adhesive layer (10 nm) and a thin Cu film (200 nm) were thermally evaporated on bare quartz crystal resonators (10 MHz, AT cut, Vectron International). Software written in the lab was coupled with a Saunders 250B Network Analyzer PCI computer card (Saunders & Associates Inc.) to monitor the admittance of the quartz, extracting the resonance frequency f and the damping parameter w (full width at half height of the admittance peak).

2.3. Scanning electron microscopy and X-ray photoelectron spectroscopy

The morphological characterization of the silicon layers was completed using an ultrahigh resolution scanning electron microscope (FE-SEM, Hitachi S-4800).

The composition of the layers was analyzed by X-ray photoelectron spectroscopy (XPS) with a Specs SAGE spectrometer (base pressure < 1×10^{-8} mbar), equipped with a Phoibos 150 electron analyzer, using focused monochromatic AlKα radiation ($h\nu$ = 1486.7 eV). The measurements were performed using analyzer pass energies of 35 eV for survey spectra and 13 eV for high-resolution spectra. These operating conditions led to a total energy resolution of 0.6 eV (FWHM of Ag 3d5/2 at pass energy of 13 eV of sputtered Ag reference sample). The absolute error in the acquisition of binding energies is 0.1 eV, as quoted by the instrument manufacturer (SPECS Surface Nano Analysis GmbH, Germany). All XPS spectra were recorded at normal emission (Θ = 0°, the angle between the surface normal and the leaving electrons) and the information depth can be estimated to be ~12 nm [25].

XPS sputter profiling was performed using a differentially pumped IQE 12/38 ion source operated with argon (source pressure 2.2×10^{-3} mbar, Ar^+ ion energy 3 keV, 10 mA emission current, 6 mA ion current) and laterally scanning the Ar^+ ions across the sample surface (scan area 10 × 10 mm^2). Under these conditions, the samples were etched at a rate of 3 nm·min^{-1} for 20 min. The core level spectra were analyzed by subtracting a Shirley-type background [26] and peak areas were calculated by a weighted least-squares fitting of model curves (70% Gaussian, 30% Lorentzian) to the experimental data using the software package CASA XPS (Version 23.16 Dev52, Casa Software Ltd.). Photoionization cross sections by Scofield were used to quantify the atomic percentage (at.%) [27]. After preparation and washing, the samples were packed into a hermetically sealed transfer box for transportation into the fast entry lock chamber. To protect the samples from moisture/air exposure, a nitrogen dry box (CarlRothGmbH, Germany) was mounted to the XPS spectrometer so that the samples could be easily removed from the transfer box within the dry box, placed in the transfer chamber and characterized at 6×10^{-8} mbar.

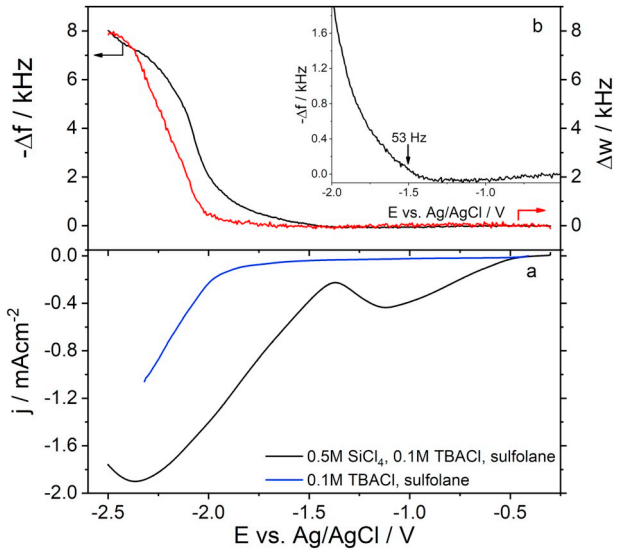

Fig. 1. Linear sweep voltammetry, measured in sulfolane containing 0.1 M TBACl and 0.5 M $SiCl_4$ (black), voltammogram measured without $SiCl_4$ in the electrolyte (blue). Scan rate of ν = 10 mVs^{-1} - (a) Frequency response (black) and damping (red) during the linear sweep - (b) Inset: enlarged view of the onset of the frequency change. Potential is referred against Ag/AgCl (0.1 M TBACl, sulfolane). (For interpretation of the references to color in this figure legend, the reader is referred to the web version of this article.)

3. Results and discussion

3.1. Electrochemical deposition of silicon

In order to determine the potential range of Si deposition in sulfolane, linear sweep voltammetry was performed, coupled with QCM measurements. Fig. 1a shows the voltammetric curves, measured in 0.5 M $SiCl_4$, 0.1 M TBACl, sulfolane. According to the voltammetry the reduction process in the presence of $SiCl_4$ starts at about $E = -0.5$ V and continues with two current peaks, observed at $E = -1.12$ V and $E = -2.35$ V (Fig. 1a, black line). The reference measurement in the absence of $SiCl_4$ (blue line) shows no reduction behavior until the onset of the electrolyte decomposition at about $E = -1.75$ V. The QCM measurement performed simultaneously does not show any frequency change until $E = -1.4$ V, which suggests that the electrochemical process assigned to the peak at $E = -1.12$ V is not associated with Si deposition (Fig. 1b). Since the frequency of the quartz does not change in this potential interval, bulk deposition can be ruled out and the first voltammetric peak could be attributed to a partial reduction of $SiCl_4$ to a soluble species, Si_xCl_{4-y}. With the onset of the current increase at $E = -1.4$ V, the frequency decrease corresponds already to a mass accumulation. This indicates that the reduction to Si^0 probably starts at this potential. For more negative potentials ($E < -2$ V) the frequency undergoes a strong decrease, which is accompanied by considerable damping. The latter can be associated with deposition of a rough and/or viscoelastic layer on the quartz resonator.

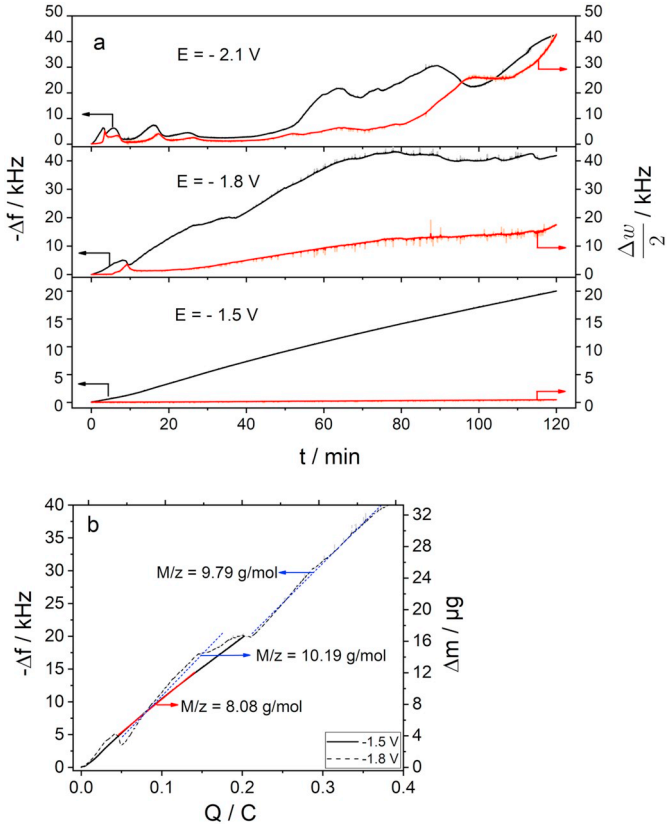

Fig. 2. Change in the frequency (black) and damping (red) during the deposition of Si from 0.5 M $SiCl_4$ in sulfolane at different potentials - (a) Frequency and mass evolution as functions of charge, during Si electrodeposition at $E = -1.5$ V and $E = -1.8$ V with estimate of the apparent molar mass - b. Potential is referred against Ag/AgCl (0.1 M TBACl, sulfolane). (For interpretation of the references to color in this figure legend, the reader is referred to the web version of this article.)

Based on the analysis of voltammetric and frequency responses, we have intentionally decided to perform a long potentiostatic deposition at very low overpotential ($E = -1.5$ V) – conditions characterized by minimal damping and the absence of electrolyte decomposition. Potentiostatic experiments were also carried out at $E = -1.8$ V and $E = -2.1$ V for comparison. The frequency response and the corresponding damping evolution for the three potentials are presented in Fig. 2a.

In order to evaluate the amount of deposited Si, the frequency response can be transformed into deposited mass by applying the Sauerbrey equation [28] (Eq. (1)):

$$\Delta f = -\frac{2f_0^2}{Z_{M,Q}}\frac{\Delta m}{A} = -C_{SB}\frac{\Delta m}{A} \quad (1)$$

Here Δf is the frequency change, f_0 – frequency of the unloaded quartz, Δm – mass change, A – mass sensitive electrode area, $Z_{M,Q}$ – mechanical impedance of the quartz crystal (8.849×10^6 kg m^2 s^{-1} for 10 MHz AT-Quartz) and C_{SB} is the Sauerbrey constant (226.01 Hz cm^2 µg^{-1}).

During the electrochemical deposition, structural effects leading to rough morphology of the interface and/or viscoelastic mechanical behavior of the layer can dissipate the energy of the oscillating system, leading to an increase in the resonance frequency damping, Δw. As a result, the response of the piezoelectric resonator displays a complex frequency shift, Δf^*, given by Eq. (2) [29], which can be used for estimation of possible energy dissipative phenomena. In Eq. (2) w and w^0 are the damping of the loaded and unloaded quartz, respectively and $i = \sqrt{-1}$.

$$\Delta f^* = f - f^0 + i\frac{(w - w^0)}{2} = \Delta f + i\frac{\Delta w}{2} \quad (2)$$

The resonance frequency signal for the measurement at $E = -1.5$ V displays an almost linear decrease and only a minimal change in damping, suggesting the formation of a smooth and rigid layer. The low damping ($\Delta f \gg \Delta w/2$) allows the application of the Sauerbrey relation (Eq. (1)) for further quantitative mass analysis [28]. Thus, the EQCM data can provide information about the amount and the supposed chemical nature of the deposit, where the apparent molar mass, M_{app}, can be calculated as follows (Eq. (3)) [30]:

$$\frac{M_{app}(E)}{z} = F\left(\frac{\partial m}{\partial Q}\right)_E \quad (3)$$

In Eq. (3) z is the number of exchanged electrons and Q the electrical charge during the deposition. Fig. 2b shows the frequency change and the corresponding mass as a function of the charge accumulated during the deposition. From the slope of the linear fit (red line) the M/z ratio for $E = -1.5$ V is calculated to be 8.08 g mol^{-1}. With the assumption of $z = 4$ for Si reduction the calculated molar mass from the EQCM experiment is $M_{QCM} = 32.32$ gmol^{-1}, which is very close to the theoretical one for Si, $M_{TH} = 28.09$ gmol^{-1}, at 100% current efficiency. Therefore, we can assume that mainly elemental Si is deposited onto the electrode. The observed small deviation is probably due to the inclusion of additional mass (e.g. electrolyte molecules or ions) in the pores of the layer. Similar behavior can be observed for the QCM measurement at $E = -1.8$ V. The frequency shift at this potential (Fig. 2a) is two times higher, reaching a plateau (≈40 kHz) after 80 min. This result suggests an inhibition of the deposition process, probably due to the low conductivity of the deposited Si. Furthermore, the increase in damping is higher than for the deposition at $E = -1.5$ V, however $\Delta f \gg \Delta w/2$ still holds, at least at the beginning of the deposition process. M/z increased slightly to approximately 10 gmol^{-1} per electron, apparently due to contamination with electrolyte components.

At more negative potentials ($E = -2.1$ V) there is no visible frequency decrease during the first 40 min, followed by strong fluctuations of the frequency and marked damping increase. This effect may be due to the decomposition of the supporting electrolyte salt. This side reaction disturbs the reduction of $SiCl_4$ leading to a low deposition efficiency. Because of the strong instability of the frequency signal at $E = -2.1$ V a reliable value for M/z could not be calculated.

Thus, for further characterization using SEM and XPS, silicon was deposited onto freshly polished copper plates at $E = -1.5$ V until a specific charge of 1C/cm^2 was reached.

3.2. Morphological characterization and chemical composition

The morphology of the Si layers was investigated by SEM imaging at two different magnifications, as shown in Fig. 3. The micrograph at the higher magnification shows a flat structure at the nanoscale, whereas at lower magnification a small number of macro defects can be detected. The thickness of the layer estimated from the cross-sectional view varies in the range from 750 nm to 1 µm (Fig. 3c). The maximum thickness of the layer depends strongly on the resistivity and, therefore, on the deposition conditions. The EQCM measurements suggest that at low overpotentials the layer mass (thickness) grows linearly until saturation, limited by the resistivity of the deposit.

XPS analysis was performed to determine the chemical composition of the deposited layer and its interface with the copper substrate. Fig. 4 presents the XPS survey spectra and the Si2p core level peaks before and after sputtering and the Cu2p spectrum after sputtering of the sample. The survey spectra (Fig. 4) reveal the presence of oxygen, carbon and silicon. In addition, minor chlorine content (0.6 at.%), which probably originates from the silicon precursor or supporting electrolyte, was detected. The absence of any trace signals from nitrogen and sulfur emphasises that sulfolane and TBACl are

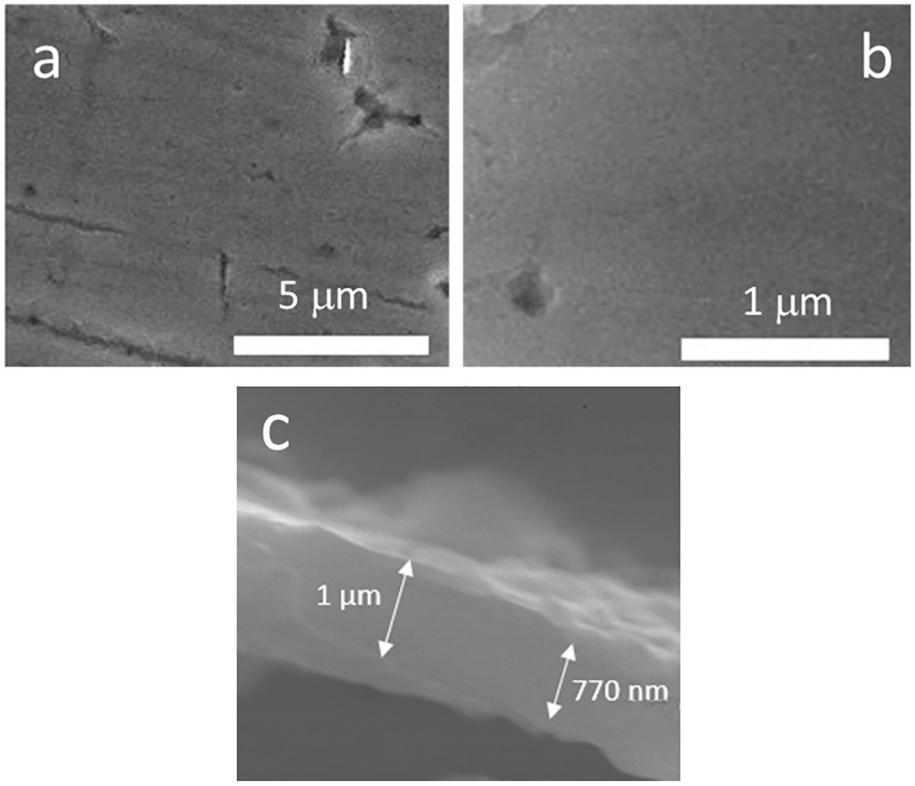

Fig. 3. SEM images of the electrodeposited silicon layer on copper substrates (a, b) - top view; (c) - cross-sectional view. Electrolyte: 0.5 M $SiCl_4$, 0.1 M TBACl in sulfolane. $E = -1.5$ V.

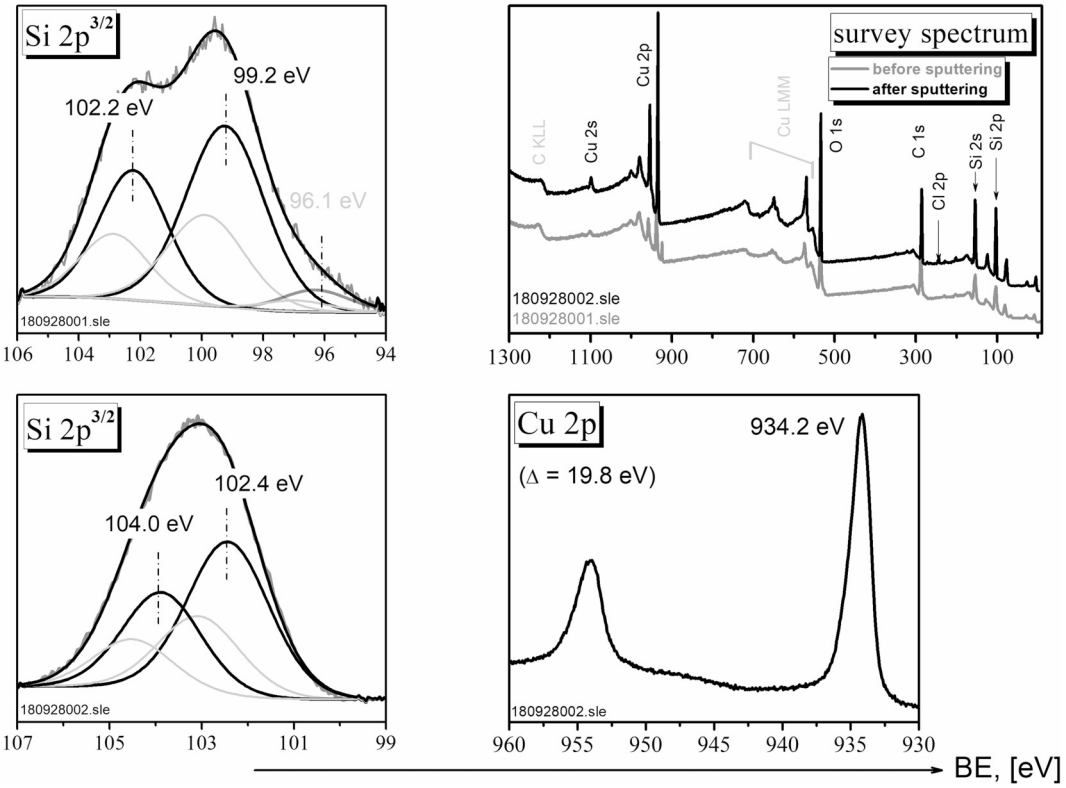

Fig. 4. Survey spectra of the electrodeposited Si layer on Cu substrate, before and after sputtering (upper right panel), $Si2p^{3/2}$ core level peaks before and after sputtering (upper left and down left panels, respectively) and the Cu2p core level peak after sputtering (lower right panel). All detected elements are depicted on the survey spectra and the deconvoluted components from $Si2p^{3/2}$ are labeled. The experimental spectra are colored in grey, the envelope peak and the $2p^{3/2}$ fitted components in black, and the $2p^{1/2}$ core levels are in light-grey. Only the experimental spectrum from Cu2p core level is shown.

electrochemically stable under the applied experimental conditions (potentiostatic deposition at $E = -1.5$ V). Furthermore, the detected oxygen signal (not shown here) corresponds mainly to C═O and C—O functional groups. These components may originate from the propylene carbonate used as a solvent for sample washing, since no C═O or C—O sources are present in the electrolyte solution.

The deconvolution of the Si2p core level peak before sputtering shows the presence of Si in two oxidation states: Si^0 and Si^{2+}, which are assigned based on the binding energy positions of $Si2p^{3/2}$ core levels [31]. It should be mentioned that to fully interpret the deconvoluted spectra of $Si2p^{3/2}$ it was necessary to consider an additional weak component (6 at.%) at 96.1 eV. Therefore, the Si^0/Si^{2+} ratio is 58:36 at. % (by considering the total amount of Si 100%).

This result shows unambiguously that elemental Si can be electrochemically deposited from sulfolane electrolyte. The total amount of silicon on the surface of the layer is 42.2 at.% and after sputtering increases slightly to 50.3 at.%. After sputtering, however, the chemical composition of the electrodeposited layer changes and the detected signals from $Si2p^{3/2}$ at 102.4 eV and 104.0 eV indicate the presence of Si^{2+} and Si^{4+}, respectively [31]. The increase in the Si oxidation state near the Cu/Si interface can be associated with the surface chemical properties of the substrate. A well-resolved spectrum from the Cu surface delivers valuable information about the chemical composition at the interface (Fig. 4, lower right panel). The binding energy position of $Cu2p^{3/2}$ core level peak at 934.2 eV implies possible presence of copper ions in three different oxidation states: Cu(0), Cu(I) and Cu(II) [32]. The absence of any shake-up peaks, which are characteristic for Cu(II) d^9 electronic state, points to the presence of a mixture of Cu(0) and Cu(I). However, the resolution and quantification of these chemical states are difficult because the overlap of the corresponding peaks requires precise constraints on BE, full-width-at-half-maximum (FWHM) and peak–shape parameters [33]. We interpret the present results as a possible formation of binary metal compounds (i.e. copper silicide) Cu_nSi, which confirms an interfacial Si–substrate reaction and give rise to very good adhesion of the deposited layers.

4. Conclusion

In this work electrochemical, microgravimetric and spectroscopic approaches are combined to investigate the deposition of silicon from a sulfolane-based electrolyte. The EQCM measurements support the suitability of this electrolyte to perform $SiCl_4$ reduction. Low resonance frequency damping and close to theoretical apparent molar mass are characteristic for the deposition at low overpotentials. It can be suggested that these experimental conditions allow the formation of thin Si layers with low roughness and minimal incorporation of organic contaminants. Due to its high reactivity, the deposited elemental silicon interacts chemically with the copper substrate to form a stable binary metal layer. It can be anticipated that the formation of covalent Cu—Si bonds contributes to the very good adhesion of the deposited silicon.

Acknowledgements

The financial support for the PhD program of Steffen Link from Cusanuswerk is gratefully acknowledged. The authors are thankful for the research funding by the State of Thuringia and the European Union within the frame of the European Funds for Regional Development (EFRD) under grant 12021–715. We acknowledge the support for the Article Processing Charge by the German Research Foundation (DFG) and the Open Access Publication Fund of the Technische Universität Ilmenau.

References

[1] S. Oda, D.K. Ferry, Nanoscale Silicon Devices, Taylor & Francis, 2016.
[2] A. Casimir, H. Zhang, O. Ogoke, J.C. Amine, J. Lu, G. Wu, Silicon-based anodes for lithium-ion batteries: effectiveness of materials synthesis and electrode preparation, Nano Energy 27 (2016) 359–376.
[3] Y.P. Zaykov, S.I. Zhuk, A.V. Isakov, O.V. Grishenkova, V.A. Isaev, Electrochemical nucleation and growth of silicon in the KF-KCl-K_2SiF_6 melt, J. Solid State Electrochem. 19 (2015) 1341–1345.
[4] A.L. Bieber, L. Massot, M. Gibilaro, L. Cassayre, P. Taxil, P. Chamelot, Silicon electrodeposition in molten fluorides, Electrochim. Acta 62 (2012) 282–289.
[5] H. Liu, L. Hu, Y.S. Meng, Q. Li, Electrodeposited three-dimensional Ni–Si nanocable arrays as high performance anodes for lithium ion batteries, Nanoscale 5 (2013) 10376–10383.
[6] H. Liu, H. Cho, Y. Meng, Q. Li, Engineering three-dimensionally electrodeposited Si-on-Ni inverse opal structure for high volumetric capacity Li-ion microbattery anode, Appl. Mater. Interfaces 6 (2014) 9842–9849.
[7] R. Epur, M. Ramanathan, F. Beck, A. Manivannan, P. Kumta, Electrodeposition of amorphous silicon anode for lithium ion batteries, Mater. Sci. Eng. B 177 (2012) 1157–1162.
[8] X. Chen, K. Gerasopoulos, J. Guo, A. Brown, C. Wang, R. Ghodssi, J.N. Culver, Patterned 3D silicon anode fabricated by electrodeposition on a virus-structured current collector, Adv. Funct. Mater. 21 (2011) 380–387.
[9] H. Nara, T. Yokoshima, T. Momma, T. Osaka, Highly durable SiOC composite anode prepared by electrodeposition for lithium secondary batteries, Energy Environ. Sci. 5 (2012) 6500–6505.
[10] J.P. Nicholson, Electrodeposition of silicon from nonaqueous solvents, J. Electrochem. Soc. 152 (2005) C795.
[11] T. Munisamy, A. Bard, Electrodeposition of Si from organic solvents and studies related to initial stages of Si growth, Electrochim. Acta 55 (2010) 3797–3803.
[12] G. Zhao, Y. Meng, N. Zhang, K. Sun, Electrodeposited Si film with excellent stability and high rate performance for lithium-ion battery anodes, Mater. Lett. 76 (2012) 55–58.
[13] J. Gobet, H. Tannenberger, Electrodeposition of silicon from a nonaqueous solvent, J. Electrochem. Soc. 10 (1988) 109–112.
[14] M. Bechelany, J. Elias, P. Brodard, J. Michler, L. Philippe, Electrodeposition of amorphous silicon in non-oxygenated organic solvent, Thin Solid Films 520 (2012) 1895–1901.
[15] S. Zein El Abedin, N. Borissenko, F. Endres, Electrodeposition of nanoscale silicon in a room temperature ionic liquid, Electrochem. Commun. 6 (2004) 510–514.
[16] C. Fournier, F. Favier, Zn, Ti and Si nanowires by electrodeposition in ionic liquid, Electrochem. Commun. 13 (2011) 1252–1255.
[17] J. Mallet, M. Molinari, F. Martineau, F. Delavoie, P. Fricoteaux, M. Troyon, Growth of silicon nanowires of controlled diameters by electrodeposition in ionic liquid at room temperature, Nano Lett. 8 (2008) 3468–3474.
[18] X. Liu, Y. Zhang, D. Ge, J. Zhao, Y. Li, F. Endres, Three-dimensionally ordered macroporous silicon films made by electrodeposition from an ionic liquid, Phys. Chem. Chem. Phys. 14 (2012) 5100–5105.
[19] J. Komadina, T. Akiyoshi, Y. Ishibashi, Y. Fukunaka, T. Homma, Electrochemical quartz crystal microbalance study of Si electrodeposition in ionic liquid, Electrochim. Acta 100 (2013) 236–241.
[20] C. Vlaic, S. Ivanov, R. Peipmann, A. Eisenhardt, M. Himmerlich, S. Krischok, A. Bund, Electrochemical lithiation of thin silicon based layers potentiostatically deposited from ionic liquid, Electrochim. Acta 168 (2015) 403–413.
[21] Y. Nishimura, Y. Fukunaka, T. Nishida, T. Nohira, R. Hagiwara, Electrodeposition of Si thin film in a hydrophobic room-temperature molten salt, Electrochem. Solid-State Lett. 11 (2008) D75.
[22] F. Martineau, K. Namur, J. Mallet, F. Delavoie, F. Endres, M. Troyon, M. Molinari, Electrodeposition at room temperature of amorphous silicon and germanium nanowires in ionic liquid, IOP Conf. Ser. Mater. Sci. Eng. 6 (2009) 012012.
[23] J. Lagovski, The Chemistry of Nonaqueous Solvents, V4: Solution Phenomena and Aprotic Solvents, Academic Press, New York, 1976.
[24] A. Saheb, J. Janata, M. Josowicz, Reference electrode for ionic liquids, Electroanalysis 18 (2006) 405–409.
[25] S. Tanuma, C.J. Powell, D.R. Penn, Calculations of electron inelastic mean free paths, Surf. Interface Anal. 26 (2004) 1–14.
[26] D.A. Shirley, High-resolution X-ray photoemission spectrum of the valence bands of gold, Phys. Rev. B 5 (1972) 4709.
[27] J.H. Scofield, Theoretical photoionization cross section from 1 to 1500 keV, J. Electron Spectrosc. Relat. Phenom. 8 (1976) 129–137.
[28] G. Sauerbrey, Verwendung von Schwingquarzen zur Wägung dünner Schichten und zur Mikrowägung, Z. Phys. 155 (1959) 206–222.
[29] V. Lyutov, I. Efimov, A. Bund, V. Tsakova, Electrochemical polymerization of 3,4-ethylenedioxythiophene in the presence of dodecylsulfate and polysulfonic anions—an acoustic impedance study, Electrochim. Acta 122 (2014) 21–27.
[30] A. Bund, R. Peipmann, Application of PEDOT layers for the electrogravimetric detection of sulphate and phosphate in aqueous media, Electrochim. Acta 53 (2008) 3772–3778.
[31] C.D. Wagner, A.V. Naumkin, A. Kraut-Vass, J.W. Allison, C.J. Powell, J.R. Rumble Jr., NIST standard reference database 20, version 3.4 (web version), http://srdata.nist.gov/xps/, (2003).
[32] M.C. Biesinger, Advanced analysis of copper X-ray photoelectron spectra, Surf. Interface Anal. 49 (2017) 1325–1334.
[33] M. Biesinger, L. Lau, A. Gerson, R. Smart, Resolving surface chemical states in XPS analysis of first row transition metals, oxides and hydroxides: Sc, Ti, V, Cu and Zn, Appl. Surf. Sci. 257 (2010) 887–898.